

INTERPRETING MEASURED MAGNETIC FIELDS OF THE BRAIN:
ESTIMATES OF CURRENT DISTRIBUTIONS

Matti S. Hämäläinen and Risto J. Ilmoniemi

Low Temperature Laboratory
Helsinki University of Technology
SF-02150 Espoo 15, Finland

REPORT TTK-F-A559 (1984)

December 1984

ISBN 951-753-362-4

ISSN 0355-7790

TKK OFFSET

INTRODUCTION

In neuromagnetism, one tries to obtain information about electrical currents in the brain by measuring the magnetic flux density at several points outside the head. Like many other inverse problems in physics, that of neuromagnetism is non-unique: there are infinitely many current distributions that can explain the measurements.

The most common method to deal with the inverse problem is to utilize a model in which the current distribution is described with a small number of parameters. However, it is often difficult to find a model that is simultaneously restrictive enough to make the problem unique and capable of describing the essential features of the current distribution. A widely used model, suitable for interpreting the simplest field patterns, is the current dipole [1]. The use of the dipole model in locating brain activity presupposes implicitly that the activity is localized in one small area (or in several separate points). Consequently, misleading results can be obtained if the assumption is not justified. In our experience, this is often the case.

In this paper, we propose a generally applicable solution to the inverse problem: minimum norm estimates for the source current distribution are developed. These are best estimates for the current, when no a priori information about the source current distribution is assumed. In this approach, one is not forced to make arbitrary assumptions about the source current.

METHODS

We shall apply estimation theory to the inverse problem of magnetoencephalography, proposing that a linear combination of magnetometer lead fields be used as an estimate for the current distribution in the brain.

The Definition of a Lead Field

Let us denote the impressed current density with \vec{J} (instead of the commonly used \vec{J}^1): $\vec{J} = \vec{J}_{\text{tot}} - \sigma \vec{E}$, where \vec{J}_{tot} is the total current density, σ is the conductivity and \vec{E} is the electric field. \vec{J} is the direct consequence of a change of other forms of energy into electrical form: it provides the 'battery' of the circuit [2, p. 212], driving volume currents ($\sigma \vec{E}$) in the conductor.

The lead field \vec{L}_i of a magnetometer at location i is defined with

$$B_i(\vec{J}) = \int \vec{L}_i(\vec{r}) \cdot \vec{J}(\vec{r}) dV, \quad (1)$$

where $B_i(\vec{J})$ is the signal of the magnetometer caused by the impressed current distribution $\vec{J}(\vec{r})$ [3,4].

Minimum Norm Estimate for the Current Distribution

Any current distribution $\vec{J}(\vec{r})$ can be considered a vector in an infinite-dimensional linear space, indexed by the individual points of the ordinary three dimensional space and by three orthogonal directions at each point. In the following, this linear space is called the current space; its vectors are denoted by simple capital letters. The corresponding three-dimensional vector fields are distinguished by a bar above the letter.

The Euclidean inner product of two vectors of the current space is defined as a volume integral of the dot product of the corresponding vector fields, viz.

$$(J_1, J_2) = \int \vec{J}_1(\vec{r}) \cdot \vec{J}_2(\vec{r}) dV . \quad (2)$$

Also the lead fields can be considered vectors of the current space. From (1) and (2), the output of a magnetometer is equal to the inner product of the current vector and the lead field vector:

$$B_i = (J, L_i) . \quad (3)$$

In other words, B_i is equal to the projection of the current vector on the lead field, multiplied by the length of the lead field vector.

A set of n magnetometer lead fields spans, in practice, an

n-dimensional subspace of the current space. Thus the magnetometers measure the projection of the current vector on the subspace. Since no information is obtained about components of the current that are orthogonal to this subspace, a natural choice for the estimate of the current distribution is the projection itself. This projection has the smallest Euclidean norm of all the current vectors that can explain B_i . Therefore, it is called the minimum norm estimate. We will denote it by \hat{J} .

By definition, \hat{J} is a linear combination of the lead field vectors L_i :

$$\hat{J} = \sum_{i=1}^n w_i L_i . \quad (4)$$

If the L_i are orthonormal, the projection vector \hat{J} is their sum weighted by the magnetometer outputs:

$$\hat{J} = \alpha \sum_{i=1}^n B_i L_i \quad ; \quad \alpha = 1 \text{ A}^2/\text{T}^2\text{m} . \quad (5)$$

Linearly independent lead fields can always be orthonormalized. If the magnetometers have been positioned symmetrically, orthonormalization can be the easiest way for calculating the current estimate. The solution can, however, be obtained more generally with the help of the pseudoinverse (See appendix A).

Let us denote the $n \times n$ -matrix formed by the lead fields by L , and the column vector formed by the measured values B_i by B :

$$\mathbf{L} = (L_1^T \ L_2^T \ \dots \ L_n^T)^T ; \quad (6)$$

$$\mathbf{B} = (B_1 \ B_2 \ \dots \ B_n)^T . \quad (7)$$

Since B_i is the inner product of the i th row of \mathbf{L} with \mathbf{J} ,

$$B_i = (L_i, \mathbf{J}) = L_i^T \mathbf{J} , \quad (8)$$

we can express the relation between the magnetometer outputs, the current distribution, and the lead fields in a concise way:

$$\mathbf{B} = \mathbf{L}\mathbf{J} . \quad (9)$$

The shortest current vector capable of explaining the magnetometer outputs can be found by multiplying the output vector \mathbf{B} by the pseudoinverse of \mathbf{L} :

$$\hat{\mathbf{J}} = \mathbf{L}^+ \mathbf{B} . \quad (10)$$

The calculation of \mathbf{L}^+ can be reduced to the determination of the pseudoinverse of an $n \times n$ -matrix, since (Appendix A):

$$\mathbf{L}^+ = \mathbf{L}^T (\mathbf{L}\mathbf{L}^T)^+ . \quad (11)$$

The components of the matrix $\mathbf{L}\mathbf{L}^T$ are the inner products between the lead fields:

$$(\mathbf{L}\mathbf{L}^T)_{ij} = L_i^T L_j = (L_i, L_j) = \int \bar{L}_i \cdot \bar{L}_j dV . \quad (12)$$

Using (11), we can relate equations (4) and (10):

$$w_j = \sum_{k=1}^n [(LL^T)^+]_{jk} B_k . \quad (13)$$

If the matrix LL^T is non-singular, i.e., the lead fields are linearly independent, the desired pseudoinverse is simply the inverse of the square matrix LL^T .

So far, no assumptions about the current distribution have been made. In practice, the current can be assumed to be zero outside a specified region of space. Since the integration in Eq. (1) can be limited to the source current area, it is evident that the integration area in Eq. (12) can be limited as well. This assumption of a restricted source area improves the current estimates.

Utilization of Potential Measurements

Far older than biomagnetism is the study of the human body with surface potential measurements. The changes in the electrical potential on the scalp are due largely to the same source currents that are responsible for the magnetic field outside the head [5]. It is thus clear that potential measurements can, at least in principle, be used to improve the quality of source current estimates.

Let V be the potential difference between two electrodes. If V is caused by $\vec{J}(\vec{r})$, the lead field $\vec{L}_E(\vec{r})$ of the electrode pair can be defined analogously with the definition (1):

$$V(\vec{J}) = \int \vec{L}_E(\vec{r}) \cdot \vec{J}(\vec{r}) dV . \quad (14)$$

We assume n magnetic field measurements $B_1 \dots B_n$ and m potential measurements V_1, \dots, V_m . Generalizing (9) we can write:

$$M = LJ , \quad (15)$$

where M is the $n+m$ -dimensional measurement vector:

$$M = (B_1 \dots B_n ; V_1 \dots V_m) \quad (16)$$

and L is the matrix composed of electric and magnetic lead fields

$$L = (L_{1,M}^T \dots L_{n,M}^T ; L_{1,E}^T \dots L_{m,E}^T)^T . \quad (17)$$

The shortest current vector capable of explaining the measured signals is obtained by multiplying the measurement vector by the pseudoinverse of L , L^+ :

$$\hat{J} = L^+ M . \quad (18)$$

In brain studies, electric and magnetic measurements give partly the same, partly complementary information [6,7]. Potential measurements provide information about radial source

currents, which give only a small contribution to the magnetic field outside the head (in the spherical model, zero contribution) [7]. Tangential source currents affect both the electrical potential and the magnetic field. By using both methods simultaneously, a better source current estimate can be obtained than by either method alone. Perhaps the greatest obstacle in this development is that, in practical conductivity geometries, the lead fields are difficult to determine [8].

RESULTS

Before applying minimum norm estimates to brain measurements, their properties were investigated with simulations.

Point magnetometers, measuring the z-component of the magnetic field, were assumed. The conductivity geometry was supposed to be such that no volume currents had to be taken into account. This assumption is valid, for example, in the case of a conducting halfspace, where the conductivity is a function of z only. The integration area (Eqs. 1, 2, and 12) was chosen to be a part of a plane parallel to the xy-plane. The restriction of the integration area means that the source current is assumed to be confined to this area.

Once the arrangement of the magnetometers had been chosen, the signal in each magnetometer was calculated from the test current dipoles. Normally distributed random numbers, representing a specified level of white noise, could be added to each signal. The effect of noise could be diminished by spatial filtering, i.e., by smoothing. Minimum norm estimates were calculated from 1) pure signals, 2) signals contaminated by noise, and 3) smoothed noisy signals.

The estimates are visualized with arrow maps, where each arrow points into the direction of the estimated current density at the center of the arrow. The length of an arrow is proportional to the current density at that point. In the figures, the

notation $\{(x_1, y_1, z_1, \phi_1) + \dots + (x_n, y_n, z_n, \phi_n)\}$ describes the test current configuration. The coordinates x_i, y_i, z_i of each dipole are given in millimeters. ϕ_i is the angle between the i th dipole and the x -axis in degrees. The locations of the test current dipoles are shown as large arrows. The magnetometers lie on the plane $z = 0$.

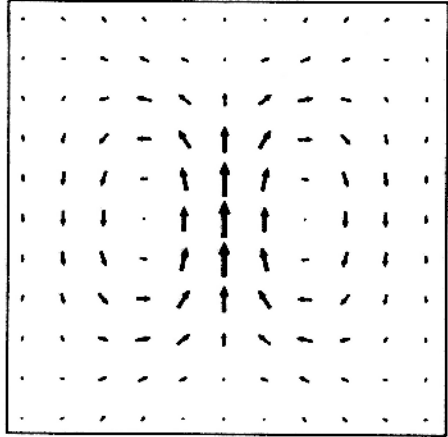
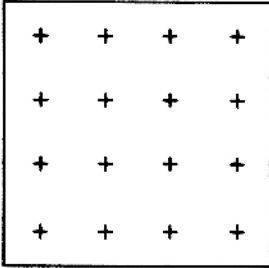
Simulations without Noise

We shall describe three sets of simulation experiments. In the first set, the area covered by the magnetometers was kept fixed, but the number of magnetometers was varied. In the second set, the number of magnetometers was fixed, but their mutual distance was varied. The third simulation tested how the structure of the test current distribution was reflected in the estimate.

In the first set of experiments 4, 9, 16, 25, and 36 point magnetometers were placed in a planar square lattice in an area of $80 \times 80 \text{ mm}^2$. The lattice constants were, thus, 80, 40, 26.6, 20, and 16 mm. The source current was assumed to be confined to a square of $200 \times 200 \text{ mm}^2$ in a plane 30 mm from the magnetometer plane. The test source was a single current dipole.

Fig. 1 shows the results of experiments with 16 and 36 magnetometers. The current estimate is more tightly localized when there are 36 magnetometers than when there are only 16 magnetometers.

a)



b)

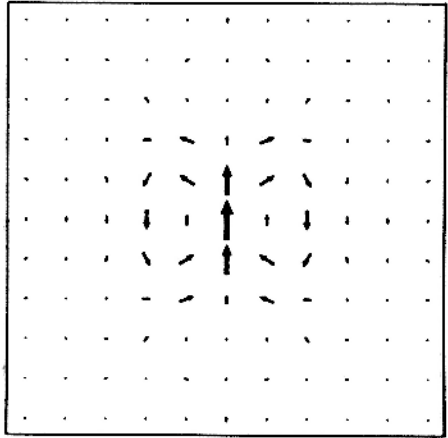
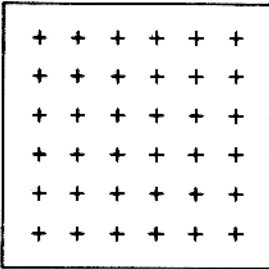


Fig. 1. The effect of the number of magnetometers on the current estimate. a) 16 magnetometers b) 36 magnetometers. Test source: $(0,0,-30,90^\circ)$. The lattice constant in the arrow map is 10 mm. The positions of the magnetometers over the source area in each case are indicated by the crosses in the separate panels.

The second set of experiments used 25 point magnetometers in a square lattice 30 mm from the source current plane. The neighboring magnetometers were 10, 20, and 30 mm from each other. The integration area and the test current were the same as in the first simulations. The results were similar to those of the first set: the estimates are best localized (confined into the smallest area) when the magnetometers are close to each other. If the dipole is located outside the area covered by the magnetometers, the estimate becomes distorted. However, even then an experimenter would get an idea about the location of the source and be able to move the magnetometer array to cover the appropriate area.

In the third set of experiments, 25 magnetometers, separated by 20 mm from each other, were assumed. The following configurations of current dipoles were used:

- a) A dipole below the center of the magnetometer array
- b) A dipole 10 mm off the center
- c) Two opposite dipoles 30 mm apart
- d) Four dipoles on the edges of a square
- e) Four dipoles in a more complicated configuration

The current estimates are depicted in Fig. 2. We notice that the essential features of the test current configurations can be resolved by the estimates. Here, as the test sources consist of current dipoles, the maxima of the estimates for the current distribution are approximately at the sites of the test dipoles.

If the current dipole nature of the source were not assumed known prior to the measurement, the location of activity should be judged directly from the current estimates instead of using the location of equivalent current dipoles.

The Effect of Noise

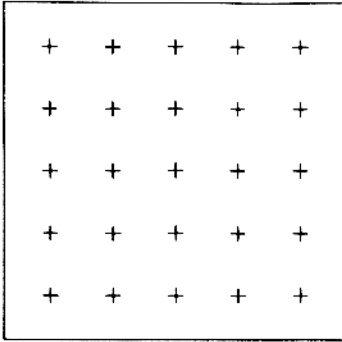
Uncorrelated noise was added to the test signals. The resulting change in the minimum norm estimates was expressed by the norm of the difference of the noisy and noiseless estimates relative to the norm of the noiseless estimate:

$$r = \frac{\|\hat{J} - \hat{J}'\|}{\|\hat{J}\|} . \quad (19)$$

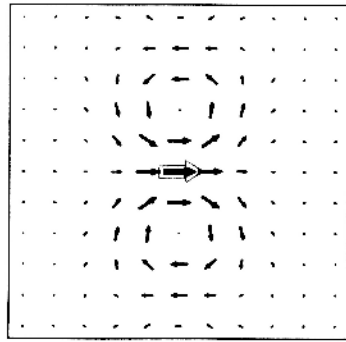
Here \hat{J} and \hat{J}' denote noiseless and noisy current estimates, respectively.

In studying the effect of noise, we assumed 25 magnetometers 10, 20, and 30 mm from each other. The current estimates were calculated for noise levels with standard deviations of 0.1, 0.5, 1, 5, 10, 20, and 50 % from the largest signal amplitude. The test source was a single current dipole 30 mm below the center of the measurement grid. The integration area for the lead fields was, like in the noiseless experiments, $200 \times 200 \text{ mm}^2$ directly below the magnetometer grid, 30 mm from it.

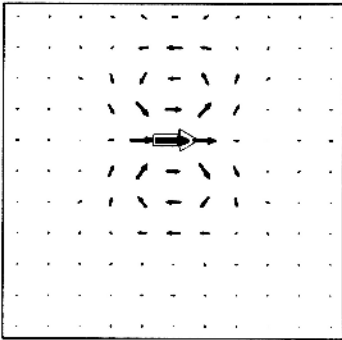
a)



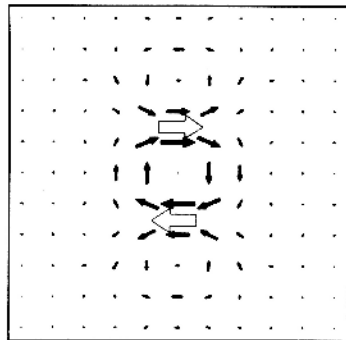
b)



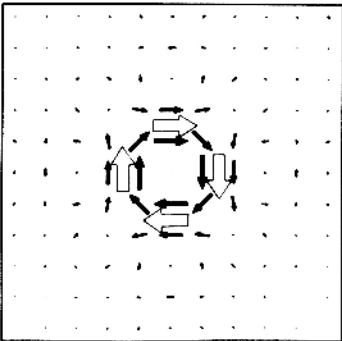
c)



d)



e)



f)

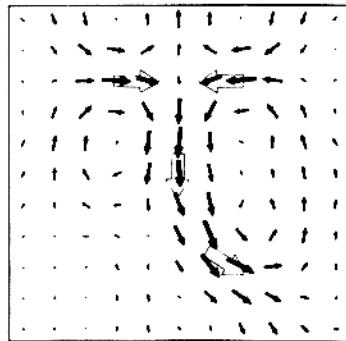


Fig. 2. Estimates from signals that originated from various source configurations. The lattice constant in the arrow map is 10 mm. Panel a) shows the configuration of the magnetometers. The following test source configurations, depicted with the large arrows, were used: b) $(0,0,-30,0^\circ)$, c) $(0,10,-30,0^\circ)$, d) $(0,15,-30,0^\circ) + (0,-15,-30,180^\circ)$, e) $(0,15,-30,0^\circ) + (15,0,-30,-90^\circ) + (0,-15,-30,180^\circ) + (-15,0,-30,90^\circ)$, f) $(-15,30,-30,0^\circ) + (15,30,-30,180^\circ) + (0,0,-30,-90^\circ) + (15,-30,-30,-45^\circ)$.

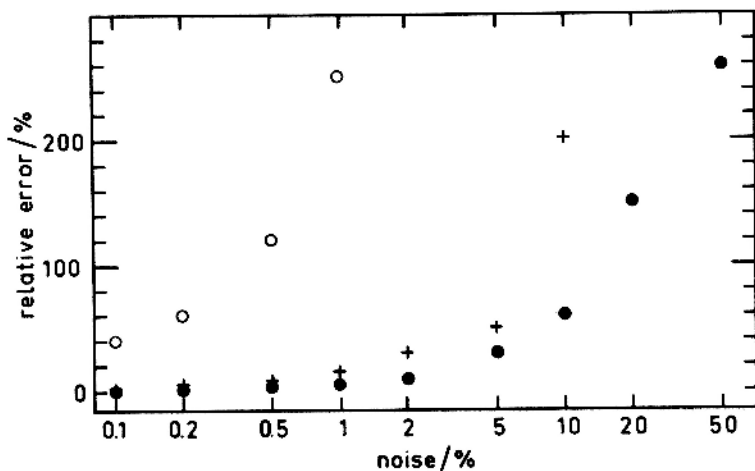


Fig. 3. The norm of the difference of noisy and noiseless current estimates relative to the norm of the noiseless estimate. The test current source is a single dipole. The 25 magnetometers are separated by 30 (●), 20 (+), and 10 mm (○).

Fig. 3 shows the effect of noise on current estimates, when the magnetometers are 20 mm apart. We notice that the noise levels of 1 % and 5 % are still acceptable, but 10 % and 20 % are not.

Simulations also indicated that:

- 1) The closer to each other the magnetometers are placed, the smaller is the level of noise that is sufficient to ruin the estimates.
- 2) For each magnetometer separation, there is a typical noise threshold, below which the current estimate is only slightly contaminated by noise, but above which the quality of the estimate deteriorates quickly. The noise threshold for the separations 10, 20, and 30 mm is about 1, 5, and 15 % of maximum signal amplitude, respectively (Fig. 3).
- 3) At high levels of noise, current loops that are coaxial with the magnetometers appear in the current estimates.

Since practical noise levels may easily distort the current estimates, we tried smoothing to alleviate the distortion. The method, distance weighted least-squares approximation, is described in [9]. The level of smoothing was determined with a parameter, α , which was selected so as to minimize the difference between estimates from smoothed and noiseless data. Again, the test current was a single dipole. As mentioned earlier, the maximum allowed level of noise without smoothing is

about 5 % from the signal amplitude. When smoothing is used, considerably higher noise levels are acceptable (Fig. 4).

Analyzing Evoked Responses

We applied the estimation procedure to somatosensory evoked magnetic fields. Following an electric stimulus to the median nerve of the left wrist, the radial field component over the right side of the head was measured with a first-order gradiometer (noise level $30 \text{ fT}/\sqrt{\text{Hz}}$) [10]. The pickup coil was about 13 mm from the scalp. For each point of the magnetometer grid, 70 to 100 responses were averaged. Since the diameter of the pickup coil was only 15 mm, and the baseline was relatively long (57.5 mm), we could approximate the device as a point magnetometer.

Fig. 5 shows field maps [10] and minimum norm estimates for various latencies. The baseline for each field value is the average value during 300 ms prior to the stimulus. 30 ms after the stimulus a clearly dipolar field pattern has emerged. At 60 ms, we get a localized estimate for the source current, although only one clear extremum is seen in the isofield contour map.

Before calculating the current estimates, the values in each field map were smoothed ($\alpha = 1000 \text{ m}^{-2}$). To calculate the inner products between magnetometer lead fields, the magnetometers were

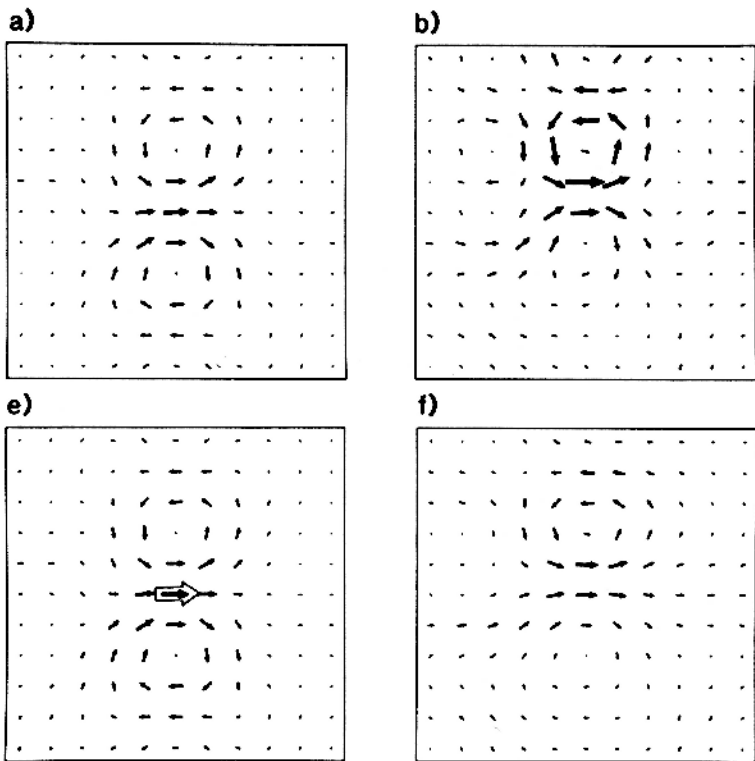
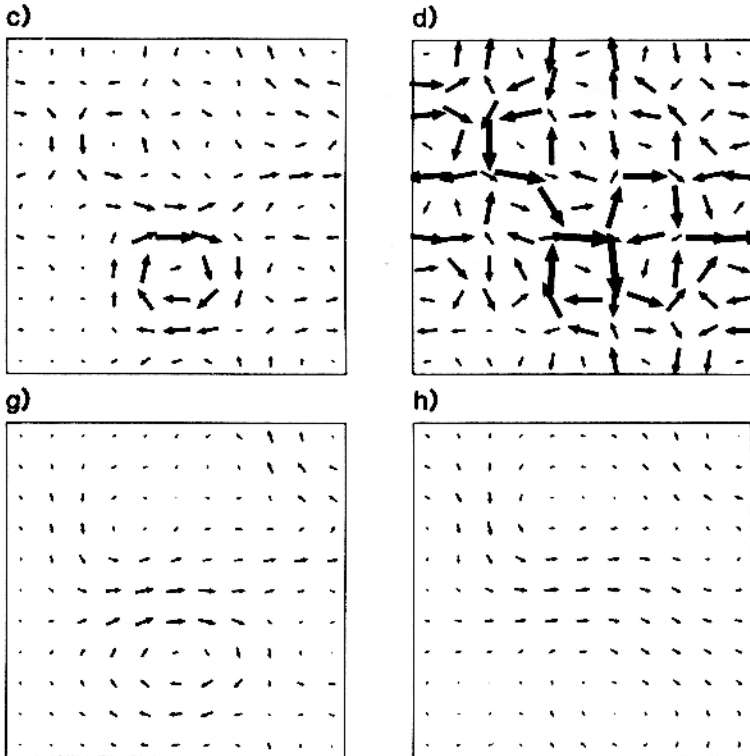
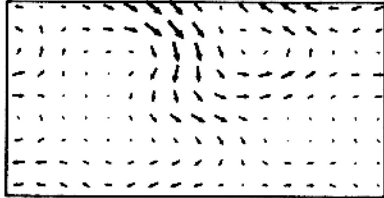


Fig. 4 a)...d) The effect of noise on current estimates.
The lattice constant is 10 nm. e)...h) Current estimates

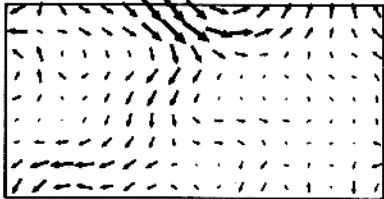
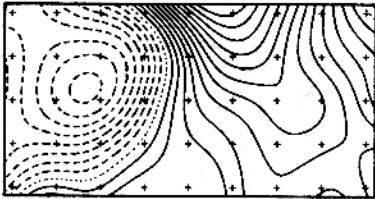


from smoothed noisy signals. The array of magnetometers is as in Fig. 3.

a) t 30 ms



b) t 60 ms



c) t 90 ms

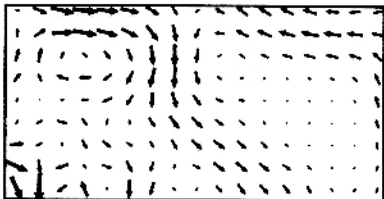
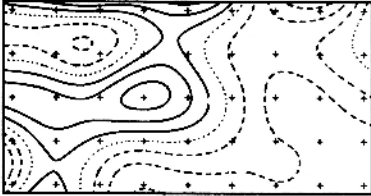
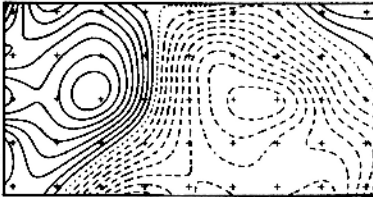


Fig. 5 a)...f) Magnetic field isocontour maps and corresponding minimum norm estimates. The separation between the contours is 50 fT. Continuous lines: flux into the head; dashed lines: flux out of the head. g) Responses from two points over the head. h) The measurement grid. The lattice constant is 2 cm.

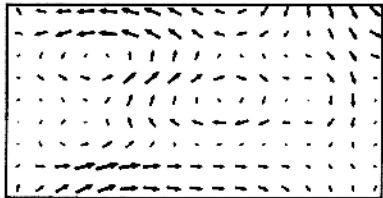
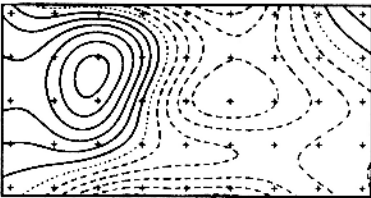
d) t 120 ms



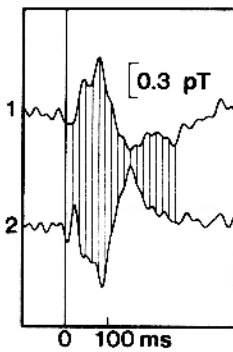
e) t 150 ms



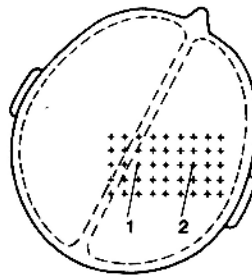
f) t 180 ms



g)



h)



assumed, for simplicity, to be situated on a plane. The integration area was chosen to be 35 mm from the magnetometer plane and to extend 10 mm from each side of the magnetometer grid.

The minimum norm estimates at the latencies 30, 60, and 90 ms are localized, with a resolution of the order of 1 cm, near the central sulcus, about 4 cm from the midline. This agrees with the known location of the sensory projection area of the hand. At 150 ms after the stimulus, the current has been reversed.

DISCUSSION

We have applied estimation theory to the problem of determining source current distributions from measured magnetic fields. In the procedure, nothing is assumed about the source current distribution except that it is confined to a certain area, for example, the brain. In the sense of the Euclidean norm, the estimate is the shortest vector in the source current space that can explain the measurements. The error is orthogonal to the subspace defined by the lead fields, i.e., there is no information about the error in the measurement signals. So the only possible way to improve the estimate is to provide some additional information. An example of the use of additional information is the assumption of the dipole model in interpreting evoked responses. This assumption is usually quite arbitrary, and it is often made only because it is felt that some model has to be assumed. It would be desirable to improve the minimum norm estimates by finding ways to inject some a priori knowledge or assumptions of the experimenter. For example, one could confine the integration area to be the cortex, or one could require that the event in the brain be local. We emphasize that one should make only those assumptions that are justified by prior knowledge. The strong assumptions implicit in the dipole model are often not well-founded. Consequently, gross misinterpretations may ensue.

We feel that minimum norm estimates are better than magnetic isocontour maps in expressing the results of magnetic field

measurements. The magnetic field is only a medium that conveys information from the brain. Since we are primarily interested in the distribution of activity in the brain, we should express our results in the form of activity distributions, i.e., source current distributions. In the transformation of data into minimum norm estimates, no information is lost, it is only transformed into another form. Even if one wants to use some dipole model, the minimum norm estimate can be the starting point. For example, one might guess from the maxima of Fig. 2 f where some current dipoles might be.

The simulation experiments show that our estimates can fairly well describe the structure of the current distribution. By increasing the number of magnetometers the estimate can be made more localized. If the actual current lies outside the area covered by the magnetometer array, the estimate is distorted.

The quality of the estimates from noisy measurements was poorest when the magnetometers were closest to each other. The effect of noise could be reduced by spatially smoothing the magnetometer outputs. After this, the highest tolerable level of noise was about 10 % of the maximum signal amplitude. Smoothing resulted in a somewhat reduced amplitude for the current estimate.

The noise level in typical evoked field studies was found to be about 10 % of the maximum signal amplitude (Appendix C). Consequently, minimum norm estimates can be applied successfully

to evoked field studies, provided that the signals are smoothed appropriately before the determination of the estimates.

ACKNOWLEDGEMENT

We are grateful to Olli Lounasmaa for continuous encouragement and support. We also wish to thank Heikki Haario, Lassi Päivärinta, Jukka Sarvas, and Erkki Somersalo for discussions and suggestions. We gratefully acknowledge Riitta Hari, Kalevi Reinikainen, and Elina Kaukoranta for the neuromagnetic measurements.

APPENDIX A

Concepts of Estimation Theory

Let $\mathbf{x} = (x_1, x_2, \dots, x_m)^T$ be a parameter vector describing some object that we investigate by measuring the vector $\mathbf{z} = (z_1, z_2, \dots, z_n)^T$, whose components are linear functions of \mathbf{x} :

$$z_i = \sum_{j=1}^m h_{ij} x_j, \quad (\text{A.1})$$

or

$$\mathbf{z} = \mathbf{H}\mathbf{x}, \quad (\text{A.2})$$

where $(\mathbf{H})_{ij} = h_{ij}$.

Noise in the measurement can be described by adding a random error v_i to each measured value z_i . An estimate $\hat{\mathbf{x}}$ is said to be **unbiased**, if its expectation value is equal to the value of the parameter vector, or $E(\hat{\mathbf{x}}) = \mathbf{x}$. For an errorless measurement, $v_i = 0$, an unbiased estimate would give the actual value of the parameter vector.

A **linear estimator** is one with the property of being a linear combination of the components of the measurement vector.

The **Moore-Penrose pseudoinverse**, or simply the pseudoinverse, is a generalization of the inverse of a matrix [11, pp. 19-32]. It is defined also for singular and non-square matrices: For

every matrix \mathbf{H} there is the pseudoinverse

$$\begin{aligned} \mathbf{H}^+ &= \lim_{\delta \rightarrow 0} (\mathbf{H}^T \mathbf{H} + \delta^2 \mathbf{I})^{-1} \mathbf{H}^T \\ &= \lim_{\delta \rightarrow 0} \mathbf{H}^T (\mathbf{H} \mathbf{H}^T + \delta^2 \mathbf{I})^{-1} . \end{aligned} \quad (\text{A.3})$$

Let \mathbf{z} be an arbitrary n -dimensional vector. $\hat{\mathbf{x}} = \mathbf{H}^+ \mathbf{z}$ is the shortest vector that minimizes the Euclidean norm $\|\mathbf{z} - \mathbf{H}\mathbf{x}\|^2$. Note that the vector \mathbf{x} that minimizes $\|\mathbf{z} - \mathbf{H}\mathbf{x}\|^2$ is unique only if $\mathbf{H}^+ \mathbf{H} = \mathbf{I}$. Then the only solution of $\mathbf{H}\mathbf{x} = \mathbf{0}$ is $\mathbf{x} = \mathbf{0}$, i.e., only the null vector is mapped to zero by \mathbf{H} .

In some special cases the pseudoinverse can be obtained from the inverse:

- 1) \mathbf{H} is a non-singular square matrix, $\mathbf{H}^+ = \mathbf{H}^{-1}$.
- 2) The rows of \mathbf{H} are linearly independent, $\mathbf{H}^+ = \mathbf{H}^T (\mathbf{H} \mathbf{H}^T)^{-1}$.
- 3) The columns of \mathbf{H} are linearly independent, $\mathbf{H}^+ = (\mathbf{H}^T \mathbf{H})^{-1} \mathbf{H}^T$.

For every matrix \mathbf{H} : $(\mathbf{H}^+)^+ = \mathbf{H}$, $(\mathbf{H}^+)^T = (\mathbf{H}^T)^+$, and $\mathbf{H}^+ = \mathbf{H}^T (\mathbf{H} \mathbf{H}^T)^+ = (\mathbf{H}^T \mathbf{H})^+ \mathbf{H}^T$. So we notice that the calculation can always be reduced to the determination of the pseudoinverse of a symmetric matrix. It turns out that for a symmetric matrix \mathbf{H} it is sufficient to determine the pseudoinverse of the diagonal matrix \mathbf{D} , related to \mathbf{H} by

$$\mathbf{H} = \mathbf{T} \mathbf{D} \mathbf{T}^T : \quad (\text{A.4})$$

$$\mathbf{H}^+ = \mathbf{T} \mathbf{D}^+ \mathbf{T}^T . \quad (\text{A.5})$$

the pseudoinverse of $D = \text{diag} (a_1, a_2, \dots, a_n)$ is

$$D^+ = \text{diag} (a_1^+, a_2^+, \dots, a_n^+) ,$$

$$\text{where } a_i^+ = \begin{cases} 1/a_i , & \text{if } a_i \neq 0 \\ 0 & , \text{if } a_i = 0 . \end{cases}$$

To diagonalize a square matrix H one has to calculate its eigenvalues and eigenvectors. The diagonal elements of D are the eigenvalues of H and the rows of T are the eigenvectors of H . For a treatment of estimation theory, see [12].

APPENDIX B

Lead Field of a Point Magnetometer

A point magnetometer at \vec{r}_i , directed to \vec{e}_i , measures one component of the magnetic flux density at that point:

$$B_i = \vec{e}_i \cdot \vec{B}(\vec{r}_i) . \quad (B.1)$$

From the law of Biot and Savart we find B_i as a function of the current distribution $\vec{J}(\vec{r}')$:

$$B_i = \vec{e}_i \cdot \frac{\mu_0}{4\pi} \int \frac{\vec{J}(\vec{r}') \times (\vec{r}_i - \vec{r}')}{|\vec{r}_i - \vec{r}'|^3} dV' . \quad (B.2)$$

By the definition of the lead field, equation (1),

$$B_i = \int \vec{L}_i(\vec{r}') \cdot \vec{J}(\vec{r}') dV' . \quad (B.3)$$

In certain symmetrical situations [13] the volume currents do not affect the measured values; then $\vec{J}(\vec{r}')$ in (B.2) can be taken to be the impressed current. By inserting a unit current dipole, $\vec{J}(\vec{r}') = \delta(\vec{r}' - \vec{r}_0) Q_0 \vec{e}$ ($Q_0 = 1$ Am), into (B.2) and (B.3), we find:

$$\vec{L}_i(\vec{r}) = \frac{\mu_0}{4\pi} \frac{(\vec{r}_i - \vec{r}) \times \vec{e}_i}{|\vec{r}_i - \vec{r}|^3} . \quad (B.4)$$

In calculating the minimum norm estimates, one needs the dot product of lead fields. We consider magnetometers 1 and 2 at \vec{r}_1

and \bar{r}_2 , with radial sensitivity axes $\bar{e}_i = \bar{r}_i/r_i$, $i=1,2$. Then, using spherical coordinates,

$$\bar{L}_1(\bar{r}) \cdot \bar{L}_2(\bar{r}) = \frac{\mu_0^2}{16\pi^2} \frac{r^2(\cos\gamma_{12} - \cos\gamma_1 \cos\gamma_2)}{\prod_{i=1}^2 (r_i^2 + r^2 - 2rr_i \cos\gamma_i)^{3/2}}, \quad (\text{B.5})$$

where γ_i is the angle formed by the vectors \bar{r} and \bar{r}_i , and γ_{12} is the angle between \bar{r}_1 and \bar{r}_2 :

$$\cos\gamma_i = \cos\theta_i \cos\theta + \sin\theta_i \sin\theta \cos(\phi_i - \phi); \quad (\text{B.6})$$

$$\cos\gamma_{12} = \cos\theta_1 \cos\theta_2 + \sin\theta_1 \sin\theta_2 \cos(\phi_1 - \phi_2). \quad (\text{B.7})$$

APPENDIX C

The Level of Noise in Evoked Field Measurements

In evoked field studies, noise can be identified as that part of the output of a magnetometer that changes randomly from one response to the next. The noise is from the instrument, the experimental subject, and external disturbances.

To estimate the noise level in evoked field measurements, we have made use of the time-variant filter of de Weerd [14,15]. His method is a generalization of Wiener filtering: at each moment of time, an optimized frequency filter is applied. To get the noise estimate, the output of the time-variant filter was subtracted from its input (from the ordinary average). The result is what the filter estimated to be noise. In this way it is found that a typical noise amplitude is 5 to 10 % of the maximum signal amplitude (Fig. 6).

Time-variant filtering cannot be used to decide how much noise in the magnetic field maps results because of the varying alertness of the subject from session to session. Therefore, our noise estimate is a lower limit to the actual noise level.

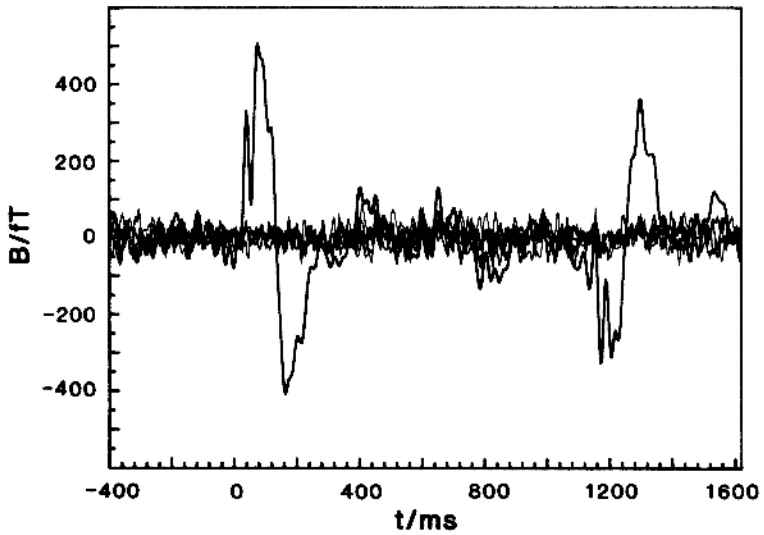


Fig. 6. Noise level in evoked field studies. The component of the magnetic field normal to the head was measured. The thick line is an average of 100 responses from the measurement location that gave the strongest signals. Electrical stimuli to the left and right wrists were applied at 0 ms and at 1050 ms, respectively. The thin lines depict noise estimates for many different measurement locations.

REFERENCES

- [1] S.J. Williamson and L. Kaufman, "Magnetic fields of the cerebral cortex," in *Biomagnetism*, S.N. Ern , H.-D. Hahibohm, and H. L bbig, eds., Berlin: de Gruyter, 1981, pp. 353-402.
- [2] R. Plonsey, *Bioelectric Phenomena*, New York: McGraw-Hill, 1969.
- [3] J. Malmivuo, "On the detection of the magnetic heart vector - an application of the reciprocity theorem," *Acta Polytech. Scand.*, EL 39, 1976, pp.1-112.
- [4] J.H. Tripp, "Physical concepts and mathematical models," in *Biomagnetism: An Interdisciplinary Approach*, S.J. Williamson, G.L. Romani, L. Kaufman, and I. Modena, eds., New York: Plenum Press, 1983, pp. 101-139.
- [5] R. Plonsey, "The nature of sources of bioelectric and biomagnetic fields," *Biophys. J.*, vol. 39, pp. 309-312, 1982.
- [6] T. Tuomisto, R. Hari, T. Katila, T. Poutanen, and T. Varpula, "Studies of auditory evoked magnetic and electric responses: Modality specificity and modelling," *Il Nuovo Cimento*, vol. 2D, pp. 471-483, 1983.

- [7] D. Cohen and B.N. Cuffin, "Demonstration of useful differences between magnetoencephalogram and electroencephalogram," *Electroenceph. clin. Neurophysiol.*, vol. 56, pp. 38-51, 1983.

- [8] B.N. Cuffin and D. Cohen, "Comparison of the magnetoencephalogram and electroencephalogram," *Electroenceph. clin. Neurophysiol.*, vol. 47, pp. 132-146, 1979.

- [9] D.H. McLain, "Drawing contours from arbitrary data points," *Computer J.*, vol. 17, pp. 318-324, 1974.

- [10] R. Hari, K. Reinikainen, E. Kaukoranta, M. Hämäläinen, R. Ilmoniemi, A. Penttinen, J. Salminen, and D. Teszner, "Somatosensory evoked cerebral magnetic fields from SI and SII in man," *Electroenceph. clin. Neurophysiol.*, vol. 57, pp. 254-263, 1984.

- [11] A. Albert, *Regression and the Moore-Penrose Pseudoinverse*, New York: Academic, 1972.

- [12] R. Deusch, *Estimation Theory*, Englewood Cliffs, N.J.: Prentice-Hall, 1965.

- [13] B.N. Cuffin, and D. Cohen, "Magnetic fields of a dipole in special volume conductor shapes," *IEEE Trans. Biomed. Eng.*, vol. BME-24, pp. 372-381, 1977.

- [14] J.P.C. de Weerd, "A posteriori time-varying filtering of averaged evoked potentials, I Introduction and conceptual basis," Biol. Cybern., vol. 41, pp. 211-222, 1981.
- [15] J.P.C. de Weerd, "A posteriori time-varying filtering of averaged evoked potentials, II Mathematical and computational aspects," Biol. Cybern., vol. 41, pp. 223-234, 1981.